Received 27 March 2020; revised 15 May 2020; accepted 16 May 2020. Date of publication 19 May 2020; date of current version 4 June 2020.
The review of this article was arranged by Editor Z. Zhang.

Digital Object Identifier 10.1109/JEDS.2020.2995710

Optimization on Adhesive Stamp Mass-Transfer of Micro-LEDs With Support Vector Machine Model

HAO LU[1], WEIJIE GUO[1], CHANGWEN SU[1], XILONG LI[2], YIJUN LU[1], ZHONG CHEN[1], AND LIHONG ZHU[1]

1 Department of Electronic Science, Fujian Engineering Research Center for Solid-State Lighting, Collaborative Innovation Center for Optoelectronic Semiconductors and Efficient Devices, Xiamen University, Xiamen 361005, China
2 Research and Development Department, Xiamen Longstar Lighting Company Ltd., Xiamen 361101, China

CORRESPONDING AUTHOR: L. ZHU (e-mail: lhzhu@xmu.edu.cn)

This work was supported in part by the Major Science and Technology Project of Fujian Province under Grant 2018H6022 and Grant 2019H6004, in part by the Natural Science Foundation of Fujian Province under Grant 2018J01103, and in part by the Science and Technology Project of Xiamen under Grant 3502Z20191015 and Grant 3502Z20173016.

ABSTRACT In this work, the process of adhesive stamp mass-transfer of micro light-emitting diode (micro-LED) is optimized by a Support Vector Machine (SVM) model. The pick-up experiments have been performed repeatedly for hundreds of times from which the separation speed and the force between the stamp and the donor substrate are extracted as signal features. The SVM model with a Gaussian kernel function is designed to classify pick-up results into success and failure. In addition, the optimal cost parameter C as well as the Gaussian kernel function parameter gamma (γ) has been optimized, leading to the improvement of the classification by Particle Swarm Optimization (PSO) algorithm. Finally, an 85% classification accuracy is achieved based on the SVM model, implying that more sophisticated definition of signal features is demanded in future work.

INDEX TERMS Adhesive stamp, mass-transfer, micro-LEDs, support vector machine model, particle swarm optimization.

I. INTRODUCTION

In recent years, micro light-emitting diode (micro-LED) has attracted a lot of attentions for its vast potential applications in various fields, such as micro-display [1]–[3], visible light communication [4]–[7], biomedical [8] and wearable devices [9]. Compared to LCD (liquid crystal display) and OLED (organic light-emitting diode) display, micro-LED display is advantageous for some unique features, including excellent light properties (e.g., contrast, hue and brightness), fast response time, high power efficiency and long lifetime [10]–[13]. However, the mass transfer process has become the bottleneck, thus hindering the mass production of micro LEDs.

A variety of mass-transfer techniques have been proposed to assemble Micro-LEDs, such as laser-Assisted mass transfer [14]–[17], fluidic self-assembly [18], [19], electrostatic mass transfer [20]–[22], micro vacuum-based transfer [8], elastomeric stamp or roll-based mass transfer [23], [24] and the adhesive stamp mass transfer adopted in this work [25]–[28]. Laser-assisted mass transfer is developed for selective micro-LEDs printing upon laser irradiation on the light-reactive layers [14]–[17]. Though good performances on the reliability, throughput, success probability as well as selectivity, this complex technique is limited to small area transfer. Fluidic self-assembly utilizes hydrodynamic interactions to achieve the assembly between the chips and the substrate [18], [19] and owns high throughput and the scalability of fluidic self-assembly. However, the reliability and the success probability are not satisfying. Electrostatic mass transfer makes use of voltage-induced electrostatic adhesion to pick up micro-LEDs from a donor substrate and release them onto a target substrate [20]–[22]. The throughput of electrostatic mass transfer is high, but LED is put at the risk of breakdown under high voltage. The micro vacuum-based transfer method picks up and releases LED chips by changing

a vacuum pressure of the transfer module, which conformally contacts LED surfaces [8]. Individual vacuum pressure control of each device enables large-scale and selective Micro-LED transfer without any adhesive and heating/compressing process. Roll-based mass transfer which developed from elastomer stamp transfer enables a large-scale, high yield and rapid transfer process for micro-LEDs display [23], [24]. However, the cost of device is high and the process is complex. Adhesive stamp mass transfer can be described as a process where a stamp picks up the ink from the donor substrate and prints the ink into the receiving substrate [25]–[29]. The stamp is typically made of molded polydimethylsiloxane (PDMS) and patterned with posts. The adhesive stamp mass transfer printing process can be achieved by utilizing the viscoelastic rate-dependent adhesion at the stamp-ink interface to enable either retrieval or printing by controlling the separation velocity [30]–[32]. Notably, the adhesive stamp mass transfer shows good reliability, high throughput, success probability, scalability of stamps and low cost, making it one of the mainstream transfer techniques. The complete transfer printing consists of the pick-up stage and the print stage. Most researches focus on the optimization of print stage. For instance, a new mode of transfer printing that utilizes a laser to supply the energy to drive a thermos-mechanical delamination process has been demonstrated by Saeidpourazar *et al.* [33], [34]. In specific, the ink is released from the stamp and then transferred to the receiving substrate. Whereas, the parameters that influence the results in the pick-up stage are rarely studied. In this work, we propose a SVM model to classify the pick-up results and optimize the pick-up stage of the adhesive stamp mass transfer technique.

In the pick-up stage, the two feature signals, namely the separation speed and the force between stamp and donor substrate, are two critical parameters that determine the success or failure in picking up chips from the donor substrate. The SVM algorithm has played an important role in the field of machine learning and attracted lots of attentions since proposed by Vapnik *et al.* for pattern recognition and data classification [35]–[37]. In this work, to distinguish whether the pick-up stage of the transferring process is successful or not, a SVM-based classifier model is demanded. We introduce Gaussian kernel function as the kernel function of the SVM based-classifier model to identify the feature signals. In order to optimize the performance, firstly, training data should include plenty of separation speed, force and the pick-up results. Based on the training data, the optimal cost parameter C as well as the Gaussian kernel function parameter gamma (γ) can be obtained with the PSO algorithm. Finally, the classification accuracy can be achieved based on the SVM model. The transfer process can be optimized by adjusting the transfer parameters of the model. In addition, both transfer yield and efficiency can be improved with the model.

II. SVM MODEL FOR MASS-TRANSFER PRINTING PROCESS

A. NORMALIZATION OF SAMPLED DATA

Signal features in the pick-up stage differ in both quantity and quality. Thus, to obtain uniformed and convergent input or output data, the sampled data should be normalized as x', varying in the range of [0, 1].

$$x' = \frac{x - x_{\min}}{x_{\max} - x_{\min}}, \tag{1}$$

where x and x' are the inputs before and after normalization respectively. $x_{\min}$ and $x_{\max}$ correspond to the minimal and maximal inputs respectively.

B. SUPPORT VECTOR MACHINE

The standard SVM algorithm is a binary classification tool, which has solved many quadratic problems with linear inequality constraints. Its explicit criteria is to find and maximize the hyperplane, which separates the two classes and minimizes the upper bound of generalization error.

When SVM is used to address non-linear inseparable samples, the original dimensional space data can be firstly mapped to a higher dimensional space, which is created by a mathematical method called kernel trick. Given a training set of S:

$$S = \left\{ (x_i, y_j) \middle| x_i \in R^N,\ \ y_j \in \{-1, 1\} \right\},\ \ i = 1, \ldots, l, \tag{2}$$

where x_i and y_j are the input and output vectors respectively. Our goal is to find an optimal hyperplane so as to separate the two classes and minimize the misclassification errors as possible. The most common way to address such problems is to transfer the original problem to a dual space using Lagrange multipliers.

$$L(\alpha) = \sum_{i=1}^{n} \alpha_i - \frac{1}{2} \sum_{i=1}^{n} \sum_{j=1}^{n} \alpha_i \alpha_j y_i y_j k(x_i, x_j), \tag{3}$$

Equation (3) is subject to the restraint as below:

$$\sum_{i}^{n} \alpha_i y_i = 0, \alpha_i \in [0, C],\ \ i = 1, \ldots, n, \tag{4}$$

where $\alpha_1, \alpha_2, \ldots, \alpha_n$are n non-negative Lagrange multipliers and $\alpha_1, \alpha_2, \ldots, \alpha_n \geq n$. $k(x_i, x_j)$ is defined as the kernel function. In this work, Gaussian kernel function is chosen as the kernel function.

$$\begin{aligned} k(x, x_i) &= \exp\left(-\|x - x_i\|^2 \Big/ 2\sigma^2 \right) \\ &= \exp\left(-gamma * \|x - x_i\|^2 \right). \end{aligned} \tag{5}$$

The SVM with a Gaussian kernel function has two training parameters, namely the optimal cost parameter (C) and the Gaussian kernel function parameter (γ). The former controls overfitting of the model and the latter determines the degree of nonlinearity.

C. PARAMETER OPTIMIZATION

According to Equations (4) and (5), the classification performance of the SVM model depends on C and γ. To improve the classification, the PSO algorithm is employed to optimize the parameters of the SVM model. The PSO algorithm searches for the optimal solution by iteration and evaluates the quality of the optimized value based on the fitness function [38], [39]. The global optimal can be achieved by utilizing the local optimal value. Normally, the velocity (v) and position (x) of each particle can be indicated as,

$$\begin{aligned} v_{i,d}(t+1) &= w \times v_{i,d}(t) + c_1 \times rand_1 \times \left(pbest_d(t) - x_{i,d}(t)\right) \\ &\quad + c_2 \times rand_2 \times \left(gbest_d(t) - x_{i,d}(t)\right), \\ x_{i,d}(t+1) &= x_{i,d}(t) + v_{i,d}(t+1), \end{aligned} \tag{6}$$

where $v_{i,d}(t+1)$ denotes the velocity of the particle i at the d-th iteration and $x_{i,d}(t+1)$ denotes the position of the particle i at the d-th iteration. w is the inertia weight that controls the impact of the velocity at previous step. t is the iteration number. c_1 and c_2 are the non-negative learning factors. $rand_1$ and $rand_2$ are random numbers in the range of [0, 1] as the remembrance ability. $pbest_d$ and $gbest_d$ respectively denote the position of the local optimal solution and the global optimal solution of the particle i after d-th iterations.

In this work, the separation speed and the force between stamp and donor substrate have been selected as signal features after hundreds of pick-up experiments and therefore the input vector in Equation (3). The pick-up result can be regarded as the output vector. Random sets of vectors were employed as the training sets for the optimization of cost parameter C and the kernel function parameter γ, the other sets of vectors as the testing sets. Given the signal features, the Libsvm toolbox in MATLAB was used to optimize C and γ of the SVM model. During the optimization, the particle swarm optimization algorithm code was invoked. The steps of optimizing the C and γ by the PSO algorithm are as follows:

1. Initialize the particle population as well as PSO parameters. According to Equation (6), set the learning factors c_1 and c_2, the inertia weight w and the max iteration number.

2. Update the positions along with the velocities according to Equation (6).

3. Evaluate the quality of the PSO optimization value by the fitness function. Then calculate the fitness value of the particle, with which the position of the local optimal solution $pbest_d$ and the global optimal solution $gbest_d$ in Equation (6) are updated correspondingly.

4. Exit the process when the maximal iteration number or the convergence accuracy is satisfied and achieve the global optimal solution $gbest_d$. Otherwise, continue the process by restarting from step (2).

The flow chart of employing the PSO algorithm to optimize the cost parameter and the Gaussian kernel function parameter of the SVM model is shown in Figure 1.

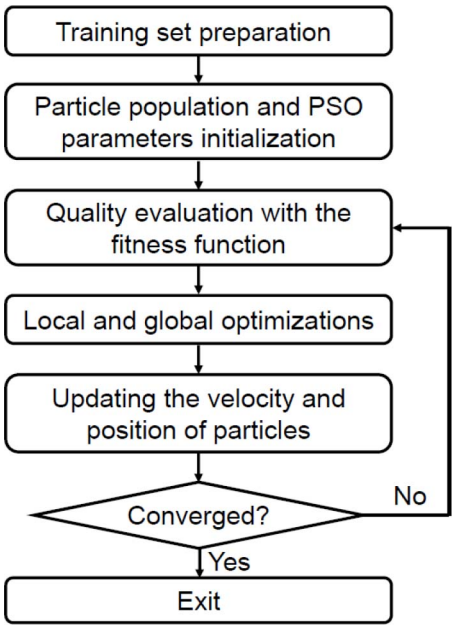

FIGURE 1. The flow chart of obtaining the optimal cost parameter C and the Gaussian kernel function parameter γ, using the PSO algorithm.

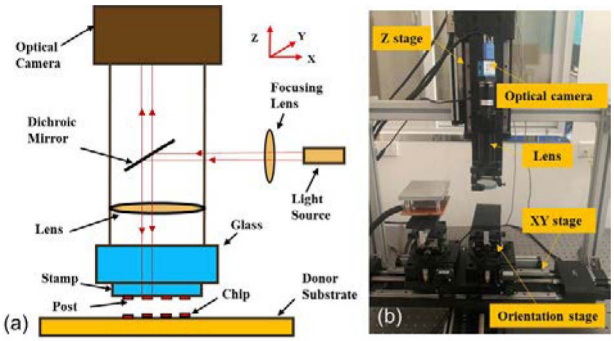

FIGURE 2. The apparatus of the mass-transfer printing system.

III. EXPERIMENTAL DETAILS

As shown in Fig. 2, the mass-transfer printing system consists of a XY-stage, a Z-stage, an orientation stage and an optical camera. The positioning resolution of XY-stage is 0.625μm. The stamp moves up and down along the Z-stage so as to touch or detach the LED chips. The GaN-based filp-chip LEDs used in the transfer experiment are supplied by Xiamen Changelight Co. Ltd, an LED fabricator. The LED wafer was grown on sapphire substrate with InGaN/GaN multiple quantum wells and the emission wavelength is about 460nm. The flip-chip LED chips were fabricated and packaged by regular chip process with size of $100 \times 200\mu m^2$. The force between stamp and donor or receiving substrate is controlled by the separation speed. The orientation stage plays a key role in obtaining parallel alignment between the stamp and the donor or receiving substrate.

In the pick-up stage, the picking results are affected mainly by two factors, namely the separation speed and the force between stamp and donor substrate. The former is controlled

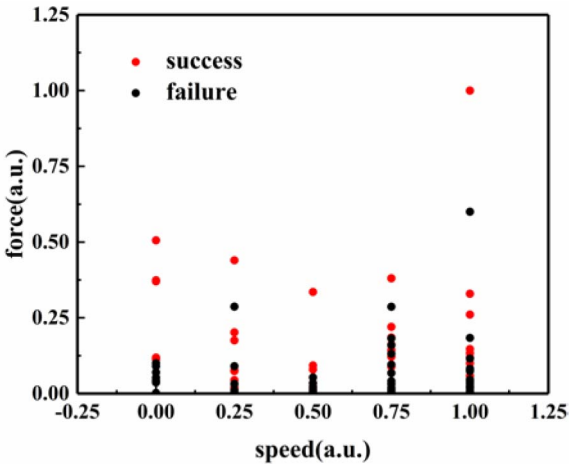

FIGURE 3. The normalized training data include the separation speed data and force data between the stamp and the donor substrate.

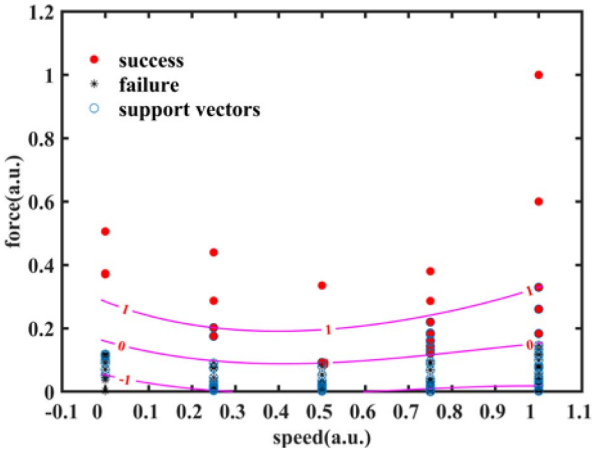

FIGURE 4. The visualizing classification result.

by the motion controller and the latter is indicated by the pressure sensor. In our experiment, a self-developed software is applied to control the motion controller of the transferring system, including the displacement of XY-stage, the Z-stage, the orientation stage and the optical camera. In details, a LED chip is placed on the donor substrate each time. The distance between the stamp and the camera is adjusted to focus on the post. Then the print head moves down along the Z-stage till the LED chip is focused and touched. The motion controller adjusts the XY-stage to parallelly align the post and the LED chip and governs the Z-stage to separate the LED chip from the donor substrate by the post. The stamp and the donor substrate are subjected to a certain pressure, being recorded by a pressure sensor. The forces and separation speed are selected and recorded as the pick-up results. Here, 1 denotes a successful pick while -1 a failure. The entire process presented above is monitored by the optical camera.

IV. RESULTS AND DISCUSSION

Signal features in the pick-up stage could differ in both quantity and quality. Thus, to obtain more uniform and convergent input or output data, the separation speed data and force data between the stamp and the donor substrate are normalized. The result is shown in Fig. 3. The training data in Fig. 3 are used to build SVM model. Then the classification was improved with the PSO algorithm where parameters C and γ are set 27 and 1 respectively. The visualizing classification result of the training data set is shown in Fig. 4. From Fig. 4, it's found that there is one data point considered as a failure during the training being classified as a success after the SVM classification, which is possible since the achievable prediction accuracy is lower than 100%.

To classify the result of the pick-up stage, the decision boundary is marked as 0. As illustrated in Fig. 4, 1 and -1 mark two curves locating at the up and down side of 0 respectively. According to the SVM algorithm, the larger the margins of the two curves are, the better the decision boundary is. Here the support vectors determine the margin. The testing data set is brought into the SVM model and the resulting predictive accuracy is 85%. The predictive accuracy less than 100% can be used to explain why the failure point should be under the decision boundary zero whereas above one in Fig. 4. Referring to the predictive accuracy and adjusting experimental signal features to further improve the accuracy accordingly, the predictive results are able to optimize the transferring process and will benefit the mass production of micro-LEDs and the automated mass-transfer printing significantly.

V. CONCLUSION

The SVM model employed in this work has been demonstrated to be able to improve the process of mass-transfer of micro-LEDs. Here the SVM model is constructed to classify the pick-up results. The signal features in the pick-up stage, including the separation speed and the force between the stamp and the donor substrate, are extracted as key parameters for SVM model building. Then the PSO algorithm was used to improve the classification, optimizing the cost parameter C and the Gaussian kernel function parameter γ. An 85% classification predictive accuracy implies the capability of SVM model for the optimization of automated mass-transfer printing process. Thus, a very large database of the mass-transfer signal features would be able to monitor and improve the mass-transfer printing process significantly.

REFERENCES

[1] P. F. Tian *et al.*, "Characteristics and applications of micro-pixelated GaN-based light emitting diodes on Si substrates," *J. Appl. Phys.*, vol. 115, no. 3, 2014, Art. no. 033112.
[2] S. L. Zhang *et al.*, "CMOS-controlled color-tunable smart display," *IEEE Photon. J.*, vol. 4, no. 5, pp. 1639–1646, Oct. 2012.
[3] J. J. D. McKendry *et al.*, "Individually addressable AlInGaN micro-LED arrays with CMOS control and subnanosecond output pulses," *IEEE Photon. Technol. Lett.*, vol. 21, no. 12, pp. 811–813, Jun. 2009.
[4] P. Tian *et al.*, "High-speed underwater optical wireless communication using a blue GaN-based micro-LED," *Opt. Exp.*, vol. 25, no. 2, pp. 1193–1201, 2017.

[5] M. S. Islim *et al.*, "Towards 10 Gb/s orthogonal frequency division multiplexing-based visible light communication using a GaN violet micro-LED," *Photon. Res.*, vol. 5, no. 2, pp. A35–A43, 2017.
[6] Y. L. Zhang, L. Wang, K. Wang, K. S. Wong, and K. S. Wu, "Recent advances in the hardware of visible light communication," *IEEE Access*, vol. 7, pp. 91093–91104, 2019.
[7] H. C. Cao, S. Lin, Z. H. Ma, X. D. Li, J. Li, and L. X. Zhao, "Color converted white light-emitting diodes with 637.6 MHz modulation bandwidth," *IEEE Electron Device Lett.*, vol. 40, no. 2, pp. 267–270, Feb. 2019.
[8] H. E. Lee *et al.*, "Micro light-emitting diodes for display and flexible biomedical applications," *Adv. Funct. Mater.*, vol. 29, no. 24, 2019, Art. no. 1808075,
[9] H. E. Lee, J. H. Shin, S. H. Lee, J. H. Lee, S. H. Park, and K. J. Lee, "Flexible micro light-emitting diodes for wearable applications," in *Proc. Light Emitting Devices Mater. Appl.*, vol. 10940. San Francisco, CA, USA, 2019, Art. no. 109400F.
[10] S. Nakamura, "InGaN-based blue light-emitting diodes and laser diodes," *J. Cryst. Growth*, vol. 201, no. 3, pp. 290–295, 1999.
[11] S. X. Jin, J. Shakya, J. Y. Lin, and H. X. Jiang, "Size dependence of III-nitride microdisk light-emitting diode characteristics," *Appl. Phys. Lett.*, vol. 78, no. 22, pp. 3532–3534, 2001.
[12] T. Mukai, "Recent progress in group-III nitride light-emitting diodes," *IEEE J. Sel. Topics Quantum Electron.*, vol. 8, no. 2, pp. 264–270, Mar./Apr. 2002.
[13] Z. Y. Fan, J. Y. Lin, and H. X. Jiang, "III-nitride micro-emitter arrays: Development and applications," *J. Phys. D, Appl. Phys.*, vol. 41, no. 9, 2008, Art. no. 094001.
[14] T. Vasileiadis, V. Dracopoulos, M. Kollia, and S. N. Yannopoulos, "Laser-assisted growth of t-Te nanotubes and their controlled photo-induced unzipping to ultrathin core-Te/sheath-TeO2 nanowires," *Sci. Rep.*, vol. 3, no. 1, p. 1209, 2013.
[15] V. R. Marinov, O. Swenson, Y. Atanasov, and N. Schneck, "Laser-assisted ultrathin die packaging: Insights from a process study," *Microelectron. Eng.*, vol. 101, pp. 23–30, Jan. 2013.
[16] R. Miller, V. Marinov, O. Swenson, Z. Chen, and M. Semler, "Noncontact selective laser-assisted placement of thinned semiconductor dice," *IEEE Trans. Compon. Packag. Manuf. Technol.*, vol. 2, no. 6, pp. 971–978, Jun. 2012.
[17] J. Bian, L. Zhou, X. Wan, C. Zhu, B. Yang, and Y. Huang, "Laser transfer, printing, and assembly techniques for flexible electronics," *Adv. Electron. Mater.*, vol. 5, no. 7, 2019, Art. no. 1800900.
[18] K. W. L. Sasaki, P. J. Schuele, K. Ulmer, and J. Lee, "System and method for the fluidic assembly of emissive displays," U.S. Patent 2017/0 133 558, May 2017.
[19] E. J. Snyder, J. Chideme, and G. S. W. Craig, "Fluidic self-assembly of semiconductor devices: A promising new method of mass-producing flexible circuitry," *Jpn. J. Appl. Phys.*, vol. 41, no. 6B, pp. 4366–4369, 2002.
[20] A. Bibl, J. A. Higginson, H. S. Law, and H. H. Hu, "Micro device transfer head heater assembly and method of transferring a micro device," U.S. Patent 10 121 864, Nov. 2018.
[21] A. L. A. Bibl, J. A. Higginson, H.-F. S. Law, and H.-H. Hu, "Method of transferring a micro device," U.S. Patent 8 333 860, Dec. 2012.
[22] H. N. Yonekura and K. Tamagawa, "Electrostatic chuck," U.S. Patent 8 023 248, Sep. 2011.
[23] M. Choi *et al.*, "Stretchable displays: Stretchable active matrix inorganic light-emitting diode display enabled by overlay-aligned roll-transfer printing," *Adv. Funct. Mater.*, vol. 27, no. 11, 2017, Art. no. 1606005.
[24] J. Y. Kim, H.-J. Choi, and C.-S. Woo, "Nanoscale thin film transfer using elastomer-covered roll with buffer cavities," *Int. J. Precis. Eng. Manuf.*, vol. 15, no. 4, pp. 711–716, 2014.
[25] R. S. Cok *et al.*, "Inorganic light-emitting diode displays using micro-transfer printing," *J. Soc. Inf. Disp.*, vol. 25, no. 10, pp. 589–609, 2017.
[26] F. N. Ishikawa *et al.*, "Transparent electronics based on transfer printed aligned carbon nanotubes on rigid and flexible substrates," *ACS Nano*, vol. 3, no. 1, pp. 73–79, 2009.
[27] C. A. Bower, E. Menard, S. Bonafede, J. W. Hamer, and R. S. Cok, "Active-matrix OLED display backplanes using transfer-printed microscale integrated circuits," in *Proc. 60th Electron. Compon. Technol. Conf. (ECTC)*, Las Vegas, NV, USA, 2010, pp. 1339–1343.
[28] C. A. Bower, M. Meitl, and D. Kneeburg, "Micro-transfer-printing: Heterogeneous integration of microscale semiconductor devices using elastomer stamps," in *SENSORS*, Valencia, Spain, 2014, pp. 2111–2113.
[29] J. Yoon, S.-M. Lee, D. Kang, M. A. Meitl, C. A. Bower, and J. A. Rogers, "Heterogeneously integrated optoelectronic devices enabled by micro-transfer printing," *Adv. Opt. Mater.*, vol. 3, no. 10, pp. 1313–1335, 2015.
[30] M. A. Meitl *et al.*, "Transfer printing by kinetic control of adhesion to an elastomeric stamp," *Nature Mater.*, vol. 5, no. 1, pp. 33–38, 2006.
[31] X. Feng, M. A. Meitl, A. M. Bowen, Y. Huang, R. G. Nuzzo, and J. A. Rogers, "Competing fracture in kinetically controlled transfer printing," *Langmuir*, vol. 23, no. 25, pp. 12555–12560, 2007.
[32] S. Kim *et al.*, "Microstructured elastomeric surfaces with reversible adhesion and examples of their use in deterministic assembly by transfer printing," *Proc. Nat. Acad. Sci.*, vol. 107, no. 40, pp. 17095–17100, 2010.
[33] R. Saeidpourazar *et al.*, "Laser-driven micro transfer placement of prefabricated microstructures," *J. Microelectromech. Syst.*, vol. 21, no. 5, pp. 1049–1058, Oct. 2012.
[34] R. Saeidpourazar, M. D. Sangid, J. A. Rogers, and P. M. Ferreira, "A prototype printer for laser driven micro-transfer printing," *J. Manuf. Process.*, vol. 14, no. 4, pp. 416–424, 2012.
[35] V. Vapnik, "The support vector method of function estimation," *Nonlinear Modeling: Advanced Black-Box Techniques*. Boston, MA, USA: Springer, 1998, pp. 55–85.
[36] V. Vapnik, V. Vapnik, and V. N. Vapnik, *Statistical Learning Theory*. New York, NY, USA: Wiley, 1998.
[37] V. N. Vapnik, *The Nature of Statistical Learning Theory*. New York, NY, USA: Springer, 1995.
[38] J. Kennedy and R. Eberhart, "Particle swarm optimization," in *Proc. Int. Conf. Neural Netw. (ICNN'95)*, 1995, pp. 1942–1948.
[39] W. Deng, H. Zhao, X. Yang, J. Xiong, M. Sun, and B. Li, "Study on an improved adaptive PSO algorithm for solving multi-objective gate assignment," *Appl. Soft Comput.*, vol. 59, pp. 288–302, Oct. 2017.

HAO LU received the B.E. degree in computer science and technology from Central South University, Changsha, China, in 2017. He is currently pursuing the M.E. degree with Xiamen University. His current research interest focuses on mass-transfer of micro-LEDs.

WEIJIE GUO received the B.S. degree in inorganic nonmetallic materials engineering from Central South University, Changsha, China, in 2005, and the M.S. degree in materials physics and chemistry from the Fujian Institute of Research on the Structure of Matter, Fuzhou, China, in 2008. He is currently pursuing the Ph.D. degree in physics electronics with Xiamen University, Xiamen, China.

CHANGWEN SU received the B.E. degree in optoelectronic science and engineering from Jimei University, Xiamen, China, in 2017. He is currently pursuing the M.E. degree with Xiamen University. His current research interest focuses on fabrication of stamps for transfer printing.

XILONG LI, photography and biography not available at the time of publication.

YIJUN LU received the Ph.D. degree in condensed matter physics from Xiamen University, Xiamen, China, in 2000, where he is currently a Professor. His current research interests include solid-state lighting testing technology and applications.

ZHONG CHEN, photography and biography not available at the time of publication.

LIHONG ZHU received the Ph.D. degree in microelectronics and solid-state electronics from Xiamen University, Xiamen, China, in 2010, where she has been a Senior Engineer with the Department of Electronic Science since 2013. Her research interests include the III-nitride-based light-emitting diodes on materials and devices.